

## EFFECT OF LOW ALUMINUM ADDITIONS IN THE MICROSTRUCTURE AND MECHANICAL PROPERTIES OF HOT FORGED HIGH-MANGANESE STEELS

E.U. Morales-Cruz <sup>a</sup>, M. Vargas-Ramírez <sup>a</sup>, A. Lobo-Guerrero <sup>a</sup>, A. Cruz-Ramírez <sup>b,\*</sup>, E. Colin-García <sup>b</sup>, R.G. Sánchez-Alvarado <sup>b</sup>, V.H. Gutiérrez-Pérez <sup>c</sup>, J.M. Martínez-Vázquez <sup>d</sup>

<sup>a</sup> Universidad Autónoma del Estado de Hidalgo - UAEH, Área Académica de Ciencias de la Tierra y Materiales, Pachuca, México

<sup>b</sup> Instituto Politécnico Nacional - ESQIE, Departamento de Ingeniería en Metalurgia y Materiales, Ciudad de México, México

<sup>c</sup> Instituto Politécnico Nacional – UPIIZ, Departamento de Formación Profesional Específica. Zacatecas, México

<sup>d</sup> Universidad Politécnica de Juventino Rosas - UPJR, Guanajuato, México

(Received 19 September 2022; Accepted 07 February 2023)

### Abstract

In the present work, the effect of low aluminum additions and the hot forging process on the microstructure and non-metallic inclusions of high manganese steels is analyzed. Four high-manganese steels (HMnS) were prepared by adding low aluminum contents of 1.1 and 1.5 wt. % to four carbon austenitic steels with medium carbon content (0.3 - 0.4 wt% C) and manganese contents of 17 and 22 wt. Samples of the as-cast steels were hot forged to 1100 °C to obtain an overall reduction of 70 %. Microstructural evolution was studied using microscopy techniques (OM, and SEM-EDS) and X-ray diffraction measurements for the as-cast and hot forged steels. A typical grain columnar zone formed during solidification of a cast ingot was obtained in the as-cast condition, where the microstructure consisted of nonmetallic inclusions in a fully austenitic matrix. The non-metallic inclusions were identified as Al<sub>2</sub>O<sub>3</sub> and MnS particles. Thermomechanical treatment allows the formation of an austenitic microstructure characterized by twins in steels with high manganese content, while an austenitic-martensitic duplex microstructure was obtained in HMnS, which contained the lowest manganese contents. The highest tensile strength values were obtained for 17Mn-1Al steel, which had the smallest grain size and higher content of non-metallic inclusions. The hardness values were similar to those obtained in the as-cast condition.

**Keywords:** Steel; Hot forging; Manganese; Hadfield; Microstructure

### 1. Introduction

High-manganese steels (HMnS) are ferrous alloys typically containing between 15 to 30 wt. % Mn with austenitic microstructure and different contents of carbon, silicon, and aluminum. They exhibit either the transformation-induced plasticity (TRIP) or the twinning-induced plasticity (TWIP) effect [1, 2]. The latter shows an excellent combination of toughness, ductility, wear resistance, and high work hardening ability that meets the needs of different industrial sectors such as automotive, mining, railroading, and naval, among others. However, the broader application of HMnS is limited due to the difficulties related to their manufacturing and processing, which require complex procedures of thermo-mechanical treatment [3]. HMnS in the as-cast condition have an austenitic matrix with complex carbides precipitated

at the grain boundaries; however, their hardness is relatively low with an average wear resistance [4, 5]. Carbon contents higher than 0.6 wt % are required to form carbides of the (Fe, Mn)<sub>3</sub>C type and the addition of carbide-forming elements to the high-manganese steels such as chromium improves its hardness and wear resistance [6-8]. On the other hand, non-metallic inclusions primarily result from the deoxidation of the steel. Deoxidation occurs with the addition of a strong deoxidizer, typically aluminum. The most common compounds found in inclusions in commercial Al-killed steels are manganese sulfide (MnS), alumina (Al<sub>2</sub>O<sub>3</sub>), different types of spinels, and when the steel is treated with calcium, calcium sulfide (CaS), and calcium aluminates (xCaO-yAl<sub>2</sub>O<sub>3</sub>) are found. Even nitrides and carbides have been found to form in the production of micro-alloyed steels [9]. As a generalization, inclusions are harmful to the

\*Corresponding author: [alcruzr@ipn.mx](mailto:alcruzr@ipn.mx)



mechanical properties and corrosion resistance of steel. This is more so for high-strength steel for critical applications [9]. Nowadays, there is an increasing interest in the development of new Advanced High-Strength Steels (AHSS) with enhanced combinations of strength and ductility which have led to the Transformation Induced Plastic (TRIP), Dual Phase (DP), Complex Phase, and Twinning Induced Plasticity (TWIP) steels [10]. Continuous casting (CC) is one of the key technologies and an indispensable manufacturing process for the production process of TWIP and TRIP steels however, the high-manganese contents has shown to be challenging for the CC and hot strip rolling processes [11]. Aluminum and silicon are also added to the HMnS to suppress the cementite precipitation, promote solid solution strengthening, and control the stacking fault energy (SFE) of retained austenite [12]. The hot ductility is an important parameter that reflects the crack sensitivity of the slab. During the solidification process of HMnS, the formation of MnS particles and complex precipitates MnS/Ti(N,C) occurs. In addition, AlN precipitates at the grain boundary, which leads to the serious deterioration of hot ductility [13, 14].

It is a common industrial practice to apply an annealed heat treatment to dissolve the carbides into a solution followed by water quenching to obtain a fully austenitic microstructure. However, the high temperature required in the annealed heat treatment produces considerable surface decarburization and manganese loss leading to martensite formation on the surface layer [15]. Therefore, an inert atmosphere is required during the annealing heat treatment. The plasticity control of the TWIP steels is achieved by a proper selection of alloying elements and the initial microstructure modification by adequate thermomechanical treatment. Additions of alloying elements can change the austenite stability and deformation mechanism. For TWIP steels, the formation of mechanical twins competes with the formation of martensite phases ( $\epsilon$  and  $\alpha'$ ), as a result of the chemical composition, temperature, and strain-induced. Aluminum and silicon are commonly added to the TWIP steels, aluminum increases the SFE and austenite stability which leads to a suppressed influence on martensite transformation; on the other hand, silicon decreases the SFE and allows occurring the martensite transformation [16-18].

It is generally accepted that in iron-base alloys, aluminum and manganese play a role as ferrite and austenite stabilizers, respectively, during phase transformations. Specifically, higher manganese content in the alloy produces a higher proportion of austenite, unlike the ferrous alloys at low temperatures that are primarily ferrite. Furthermore, in Fe-Mn-Al alloys possessing a low concentration of

aluminum and a high concentration of manganese, a fully austenitic microstructure is preserved even at low temperatures [19]. Nevertheless, a fully ferritic microstructure can form as a result of higher aluminum content [20].

Studies have been carried out about what conditions in a thermomechanical treatment are ideal to obtain new austenitic steels with high-manganese contents that present high strength and good ductility [21, 22]. Some authors have reported that SFE energy plays a crucial role in the structure and mechanical properties of steels with high aluminum content, they are attributed to two main factors that influence the SFE, which are the chemical composition and strain temperature [23, 24]. The behavior of TWIP steels subjected to hot thermomechanical treatments with aluminum contents higher than 2 wt% has been reported [25-27]. The mechanical properties were improved, especially the elongation, due to the hardening by mechanical twinning [28-30]. To develop the manufacturing methods, it is important to determine the flow behavior of steel under hot working conditions. There is a scarcity of works reported on the effect of aluminum contents lower than 2 wt% under hot working conditions of TWIP steels [31]. Therefore, this article aims to study the effect of low aluminum additions of 1.1 and 1.5 wt% to high-manganese steels containing 17 and 22 wt% Mn on the microstructural evolution and the tensile and hardness properties in the as-cast and hot forged conditions.

## 2. Materials and Methods

### 2.1. Casting of steels

Four steels with high-manganese (Mn) content were manufactured in a vacuum induction furnace with a controlled atmosphere of argon (Ar). Steels were produced by using steel scrap, low-carbon ferromanganese, and commercial pure aluminum. All the materials were melted and homogenized at 1500 – 1520 °C. Steels were poured at 1500 °C into preheated steel molds to obtain ingots of 3 x 10 x 20 cm. The ingots were allowed to cool to room temperature with air as a cooling agent. The nominal chemical composition in the steels was analyzed by a Bruker Tasman Q4, series N0088 emission optic spectrograph, and reported values are the average of four measurements on each HMnS. Carbon, nitrogen, and sulfur content were determined by combustion analysis using a Leco C/S 744 analyzer.

### 2.2. Hot forging process

Samples of 3 x 5 x 1.8 cm of each HMnS were obtained from the as-cast ingots with a wall thickness of 18 mm. The samples were preheated to 1100 °C for



1 h before being deformed. Hot forging followed by air cooling was conducted for high-manganese steels at 1100 °C by using mechanical presses of 100 and 200-ton capacities.

The as-cast HMnS samples were hot forged in three passes to obtain the reduction ratios of 12, 25, and 33 %. The HMnS samples obtained from the last step of the hot forging process were used for the microstructural and mechanical properties evaluations.

### 2.3. Microstructural characterization

The microstructural characterization was carried out on the as-cast and hot forged HMnS samples by optical microscopy (OM), scanning electronic microscopy (SEM) with energy dispersive spectra analysis (EDS), and X-ray diffraction measurements. Standard metallography techniques (mechanical grinding and polishing followed by etching with 5 % nital) were employed to reveal the microstructure and non-metallic inclusions (NMIs) of the as-cast and deformed samples. Optical microscopy was performed on polished and etched specimens by using an optical microscope Olympus PMG-3, and the image analyzer with the software Image J 4.1. The NMIs features such as average size, particle count, and volume fraction were determined based on the standard specifications of ASTM E45 on polished surfaces. Six locations chosen as representative of the sample were examined to 100 X to obtain a reasonable estimate of inclusion variations. The grain size estimation (counting both the grain and the twin boundaries) was carried out by the linear intercept method and the basic shape parameters of Image J software [32] for six representative locations of the whole sample. The deviation standard values are reported for the optical measurements. Images and qualitative chemical analysis were determined in an SEM Jeol model 6300 and with the energy dispersive spectra analysis. The backscattering electrons technique with 25 kV and 10 A was used for image production. X-ray diffraction measurements were carried out in an X-Ray Bruker D8 Focus with monochromatic Cu  $K\alpha_1$  radiation working in  $\theta/2\theta$  configuration on the as-cast and deformed samples. The following parameters were set for data collection: angular range from 30 to 100°, step size of 0.02°, and counting time of 2° min<sup>-1</sup>.

**Table 1.** Chemical composition of the HMnS (wt%)

Steel	C	Mn	Al	Si	P	S	N	Fe
17Mn-1.5Al	0.31	16.99	1.54	0.42	0.05	0.099	0.0041	Balance
17Mn-1Al	0.28	17.6	1.17	0.33	0.08	0.010	0.0047	Balance
22Mn-1.5Al	0.31	22.02	1.45	0.31	0.06	0.010	0.0038	Balance
22Mn-1Al	0.38	22.06	1.05	0.29	0.06	0.014	0.0034	Balance

### 2.4. Mechanical properties

The mechanical properties of hardness, tensile strength, and elongation were obtained from the HMnS in the as-cast and deformed conditions. Tensile testing was carried out at room temperature using a universal testing machine United STM-10-EZ of 100 kN with 10 mm/min cross-head speed. The size and geometry of the specimens were manufactured following the specifications of standard ASTM E 8. Three specimens from each steel sample were tested for tensile test, and the average of the measurements is reported. Rockwell B hardness measurements were made on the polished surfaces of each steel sample by using a Buehler hardness tester, and an applied load of 98 N and 0.15 cm indenter under the standard specification of ASTM E18-20. At least 4 and 6 measurements were taken, and the average of the measurements is reported for each steel sample.

## 3. Results and Discussion

### 3.1. Chemical composition

The chemical composition was designated by maintaining the carbon content constant at 0.3 wt% while the manganese and aluminum were set at 17 and 22 wt% and 1.1 and 1.5 wt%, respectively. Under these considerations, the aluminum was evaluated for contents lower than 2 wt%. as it is observed in Table 1. The manganese content is within the expected for HMnS. Aluminum content is related to increasing the stacking failure energy allowing the mechanical twinning formation as the primary hardening mechanism. This behavior is obtained for aluminum additions higher than 2 wt%, reaching values up to 6 wt% [33] to the TWIP steels. The carbon content is usually lower than 1.4 wt% because during processing it is lost by decarburization, which affects the mechanical properties of the steel surface. The chemical composition analyzed in the HMnS is shown in Table 1.

The formation of alumina (Al<sub>2</sub>O<sub>3</sub>) particles is expected as the de-oxidation product of the steel due to the aluminum contents in the HMnS. Furthermore, the sulfur and manganese contents in the HMnS may produce manganese sulfide particles even at low Mn and S levels [34]. It was reported [35] for medium manganese transformation-induced plastic steel that contents higher than 10 ppm of sulfur are required to



form complex inclusions of the AlN-MnS type. On the other hand, the AlN particle formation is also expected due to the aluminum and nitrogen contents in the HMnS evaluated [35, 36].

### 3.2. Microstructural characterization

#### 3.2.1. As-cast condition

The polished microstructures of the HMnS in the as-cast condition are observed in Figure 1. A significant number of particles correspond to non-metallic inclusions and porosities. The morphology of the particles corresponds to a globular shape that is mainly attributed to NMIs of the oxide type.

Table 2 shows the particle count, the NMIs - and micro-porosities content, and their average size for the HMnS. It is observed that the 17Mn-1Al steel contains the lowest NMIs amount than other steels with the smallest particle size; however, it is observed that the average particle size is similar for the HMnS evaluated in the range of 4 to 5  $\mu\text{m}$ . Figure 1 and Table 2 show small, numerous, and rather uniformly distributed particles that correspond to endogenous inclusions. The largest inclusions are usually the most damaging, especially the hard, brittle oxide inclusions, which are often the origin of variability in steel properties [37].

The four HMnS were analyzed by SEM-EDS techniques to determine the distribution of the main elements in the matrix and the particles identified as NMIs. The results were very similar for the four steels and Figure 2 shows an SEM micrograph with its microanalysis of the 22Mn-1Al steel.

From Figure 2b a homogeneous distribution of the

main elements as a solid solution in the matrix of the HMnS is observed; this behavior was obtained for the four steels where there was no segregation of the elements. The particles observed in the micrographs of Figure 1 were analyzed by EDS and the results are observed in Figure 3 for the 22Mn-1Al and 17Mn-1.5Al steels. The micrograph of Figure 3a shows three big dark particles and a small gray particle. The big dark particles are constituted mostly by aluminum and silicon while a small gray particle located at the top of the big particle located in the middle of the micrograph also contain manganese and sulfur. The smallest gray particle contains higher concentrations of manganese and sulfur. Thus, the non-metallic inclusions are mainly formed by alumina ( $\text{Al}_2\text{O}_3$ ) and manganese sulfide (MnS). The inclusions are compounds consisting of non-metallic elements, such as oxygen, sulfur, phosphorous, nitrogen, carbon, etc. Non-metallic inclusions result primarily from the deoxidation of the steel by the addition of strong deoxidizers, typically aluminum and silicon. The most common compounds found in inclusions in steels are manganese sulfide (MnS), alumina ( $\text{Al}_2\text{O}_3$ ), and

**Table 2.** Features of the NMIs and micro-porosities contained in the HMnS

Steel	Particles count (particles $\text{mm}^{-2}$ )	NMIs and micro-porosities (%)	Particles average size ( $\mu\text{m}$ )
17Mn-1.5Al	513.1 $\pm$ 62.31	0.61 $\pm$ 0.04	5.32 $\pm$ 1.29
17Mn-1Al	405.4 $\pm$ 23.56	0.41 $\pm$ 0.11	4.8 $\pm$ 0.68
22Mn-1.5Al	525.2 $\pm$ 48.81	0.59 $\pm$ 0.22	5.01 $\pm$ 1.32
22Mn-1Al	415.6 $\pm$ 38.38	0.65 $\pm$ 0.93	5.11 $\pm$ 1.48

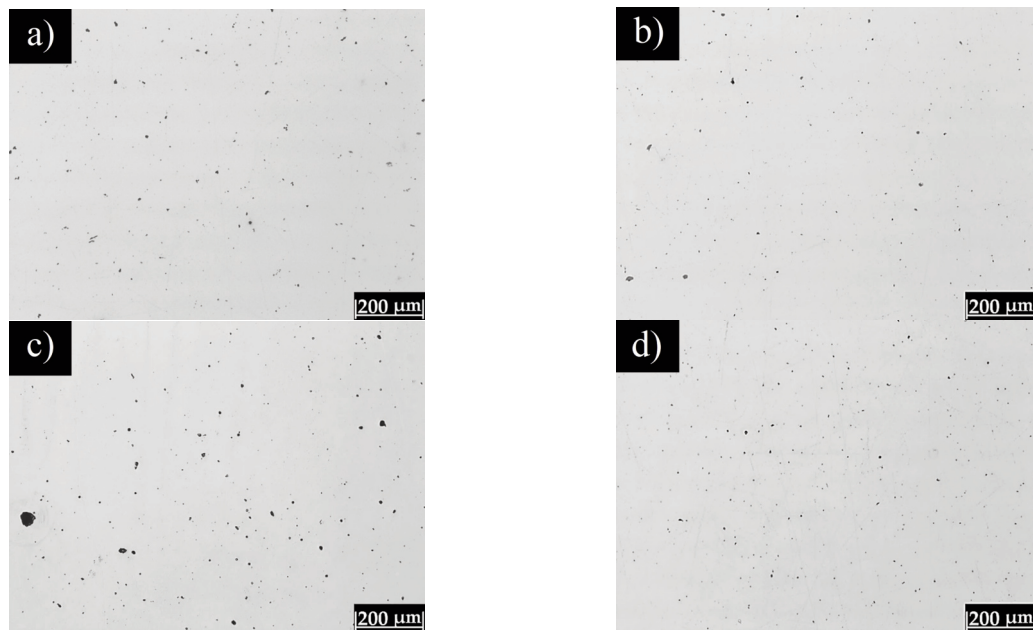


**Figure 1.** Unetched microstructures of the a) 17Mn-1.5Al, b) 17Mn-1Al, c) 22Mn-1.5Al, and d) 22Mn-1Al HMnS in the as-cast condition

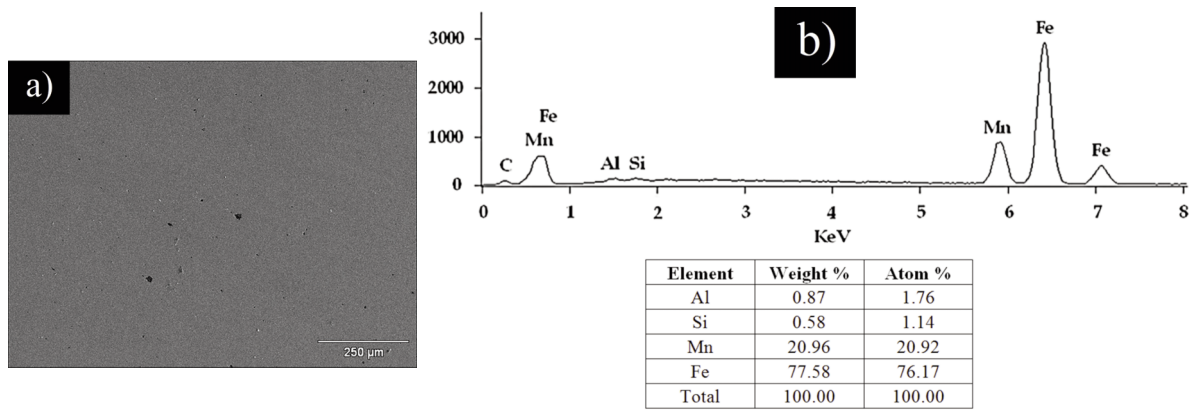


Figure 2. a) SEM micrograph and b) Punctual X-ray microanalysis of the 22Mn-1Al steel matrix

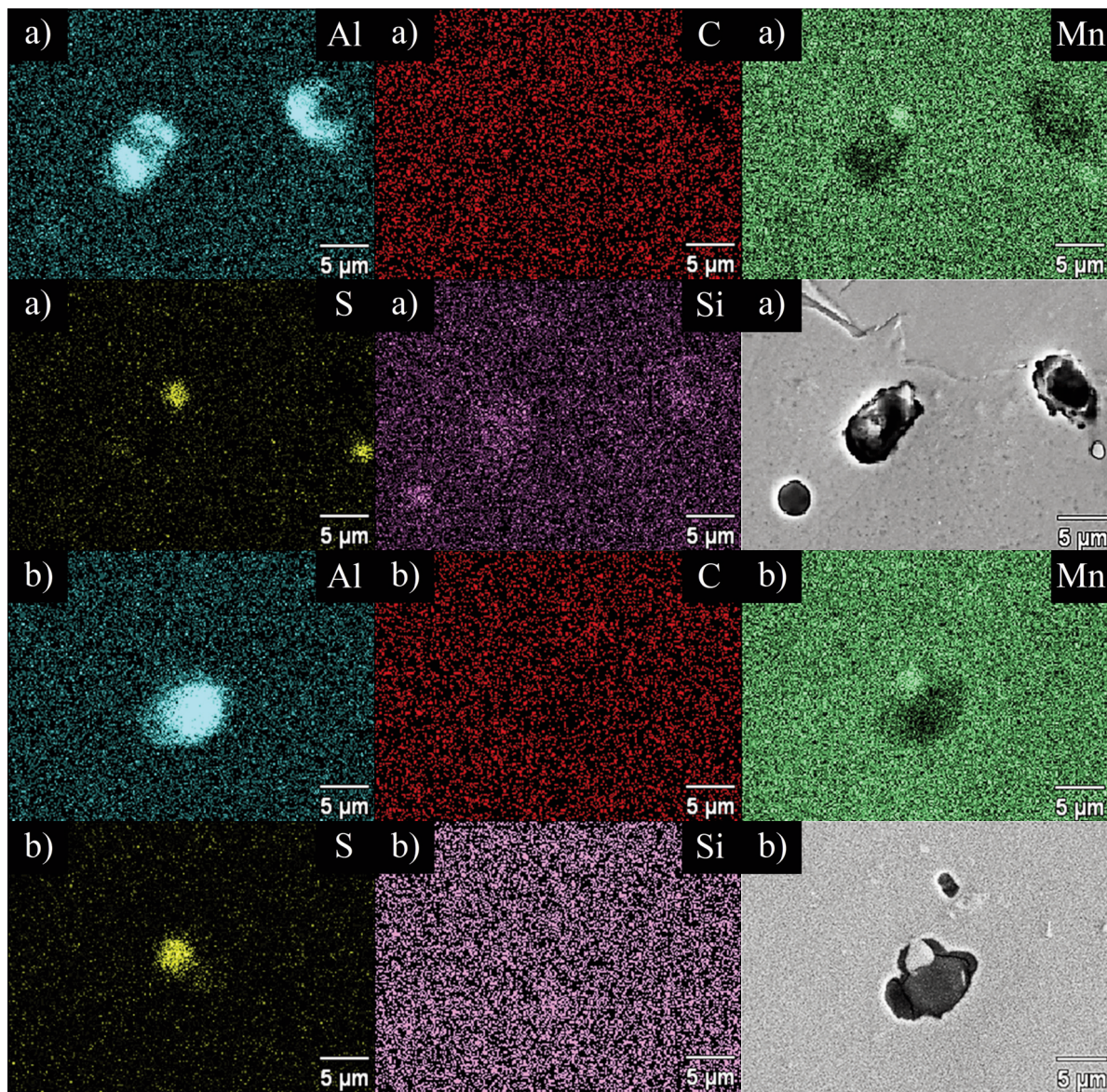


Figure 3. SEM micrograph and EDS analysis of particles contained in the a) 22Mn-1Al and b) 17Mn-1.5Al steels

different types of spinels (mainly  $\text{MgO-Al}_2\text{O}_3$ ) [9, 37].

Figure 3b shows that the NMIs are mainly constituted by alumina while the tip of the inclusion corresponds to manganese sulfide. A micro-porosity in the upper part of the micrograph is observed. It was reported that the formation of oxides is thermodynamically more stable followed by the sulfides formation in the production of ferrous alloys such as gray cast irons for lower amounts of Mn, S, and Al while the carbide formation is less stable since the thermodynamic point of view [34]. The low carbon content in the produced HMnS avoids the carbide formation as is observed in the results reported in Figure 3 where it does not observe a high-carbon concentration in the non-metallic inclusions. Therefore, the non-metallic inclusions formed during the manufacturing of these high-manganese steels correspond to alumina and manganese sulfide mainly. Nevertheless, it has been reported [35, 36] that  $\text{Al}_2\text{O}_3$  inclusions can be considered as the nucleation core of the  $\text{AlN}$  inclusions during the solidification process of Fe-0.5Al-2Mn steel. Moreover, the precipitation of MnS - and complex  $\text{AlN}$  - MnS precipitates were identified during the production of medium manganese steels (6 – 10 wt% Mn and 1 wt% Al) [36]. In this work, the presence of the  $\text{AlN}$  particles was not evident for the biggest NMIs analyzed; however, as can be observed, there is a great amount of smaller particles, especially for the 17Mn-1Al steel that could correspond to  $\text{AlN}$  inclusions.

Figure 4 shows the etched microstructure of the HMnS in the as-cast condition. The microstructure is constituted by NMIs in a fully austenitic matrix. Grain boundaries of big elongated crystals which are typically obtained during solidification of an ingot

casting in the columnar zone are observed. Figure 4c shows that the 17Mn-1Al steel has the smallest NMIs homogeneously distributed in the matrix while the other steels show bigger NMIs.

As expected, the austenitic-ferritic matrix was presented for the four steels because of their high-manganese content which led the austenite to be preserved as a metastable phase. The x-ray diffraction patterns of the HMnS are reported in Figure 5 and it is confirmed that the microstructure consists of austenite.

It is observed from Figure 5 that the main phase contained in the four steels is austenite ( $\gamma$ ) which fits with the phases reported for steels with high-manganese content. Manganese contents higher than

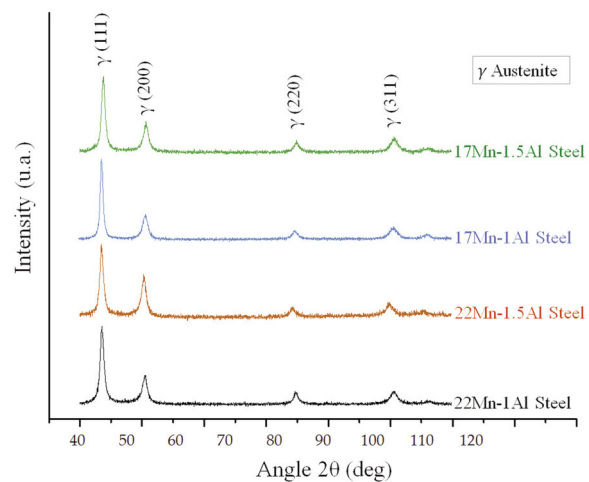


Figure 5. X-ray diffraction patterns corresponding to the HMnS in the as-cast condition

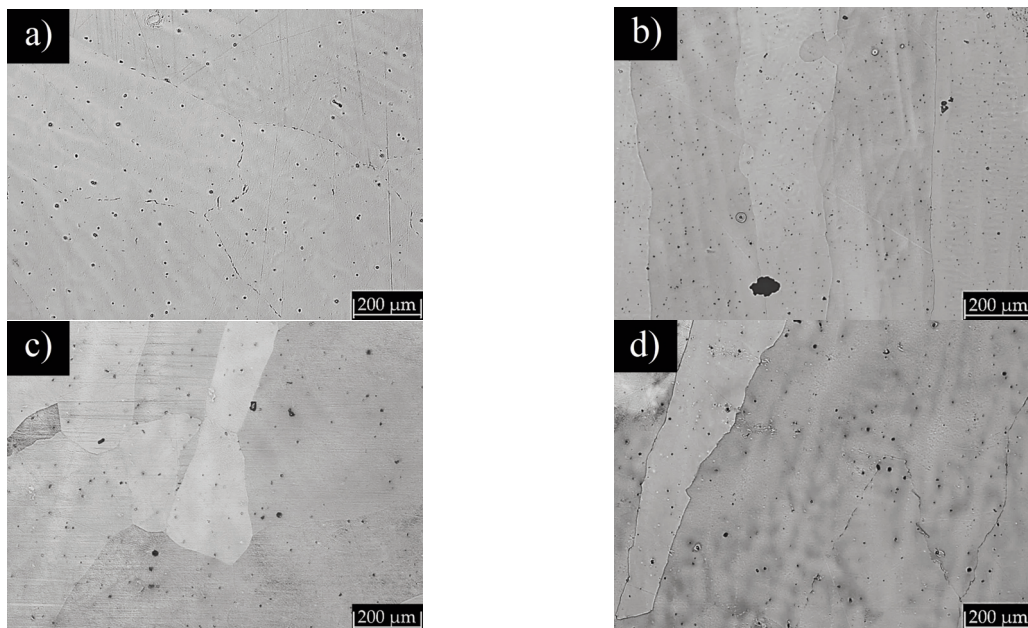


Figure 4. Etched microstructures of the a) 17Mn-1.5Al, b) 17Mn-1Al, c) 22Mn-1.5Al, and d) 22Mn-1Al HMnS in the as-cast condition

10 wt.% led to austenite ( $\gamma$ ) becoming a metastable phase at room temperature [38].

### 3.2.2. Hot forging condition

The microstructural results of the hot forged HMnS are presented in the micrographs of Figure 6 to different magnifications.

It is observed that the experimental parameters of the thermomechanical treatment allow for refining the microstructure of the HMnS obtaining equiaxed grains and NMIs from the as-cast

condition. The four HMnS show more or less equiaxed austenite grain structure with the grain size of  $68 \pm 11$ ,  $53 \pm 9$ ,  $123 \pm 13$ , and  $105 \pm 9$   $\mu\text{m}$ , for the 17Mn-1.5Al, 17Mn-1Al, 22Mn-1.5Al, and 22Mn-1Al steels, respectively, determined by the linear intercept method and the Image J software. It is evident from Table 2 that the particle average size is similar in the four steels; however, the particle count is higher when the aluminum content was increased. Therefore, the average grain size was decreased after the hot forging process because a large number of particles pinning the grain

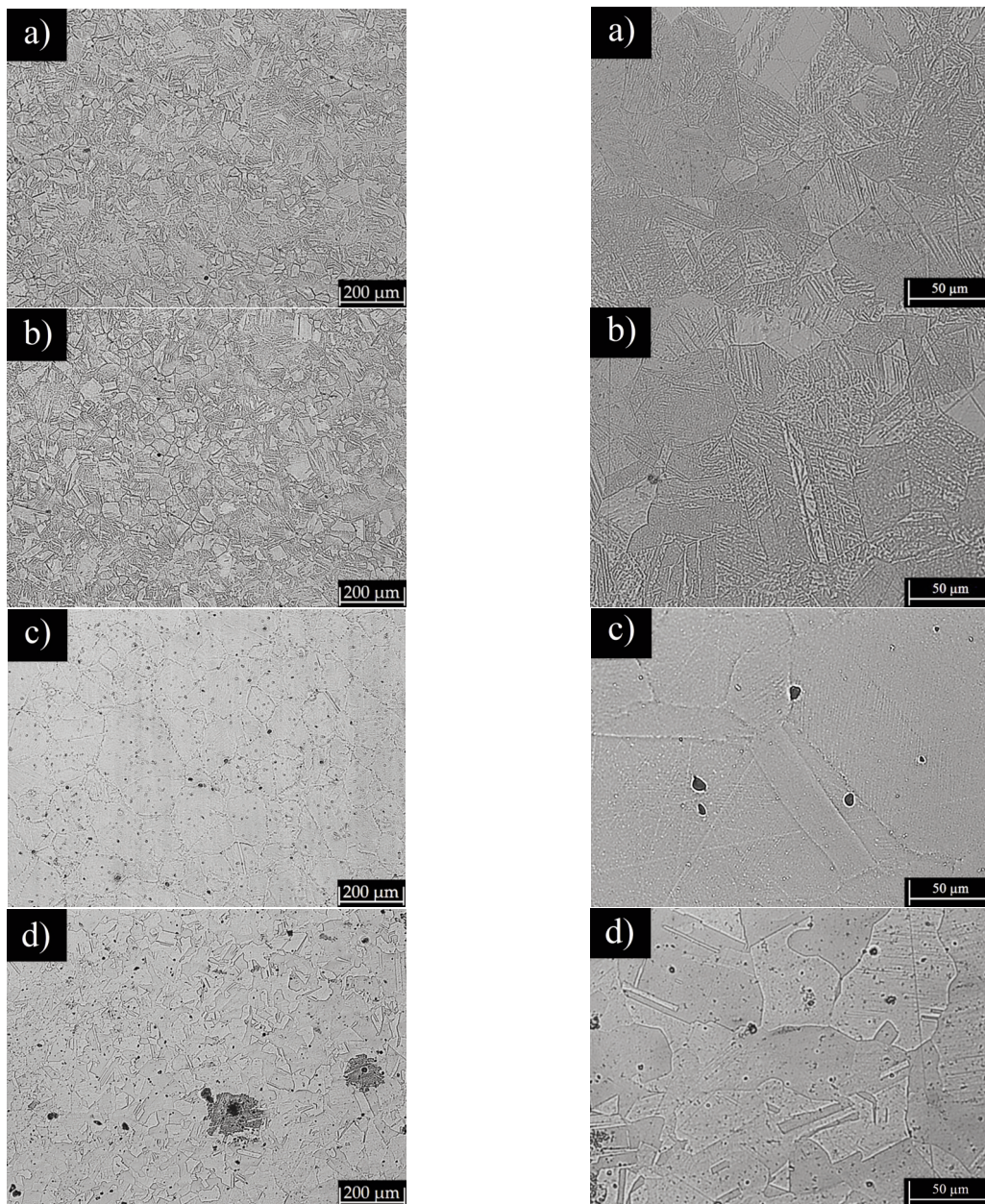


Figure 6. Microstructures of the hot forged HMnS (1100 °C, 60 min, air cooled) to a) 17Mn-1.5Al, b) 17Mn-1Al, c) 22Mn-1.5Al, and d) 22Mn-1Al

boundaries aided to refine the microstructure [39]. Z. Wu, et al [40] found that the average size grains are finer and uniform due to the large amounts of finely dispersed inclusions in a deoxidized steel containing different amounts of aluminum. Inclusions with an average size of 4.2  $\mu\text{m}$  and a high melting point inhibit the growth of austenite grains due to pinning migration of the austenite grain boundaries.

It was observed from Figure 6 that steels 22Mn-1.5Al and 22Mn-1Al show mainly a retained austenite microstructure characterized by annealing twins. However, the 17Mn-1.5Al and 17Mn-1Al steels show a duplex microstructure of martensite and retained austenite. Similar microstructures were obtained for HMnS heat treated to 1100  $^{\circ}\text{C}$  followed by water quenching [31].

The austenitic grains of the as-cast HMnS were severely deformed and dynamically recrystallized after the hot deformation process. The recrystallized grains (sub-grains) were formed near the deformed austenitic boundaries and martensitic transformation occurred in larger recrystallized austenitic grains. The optical micrograph (OM) in Figure 7a shows that the alloy grains contain irregular sub-grains within their boundaries. The micrograph in Figure 7b shows that the alloy matrix comprises martensitic laths in retained austenite grains. Martensite transformations are characterized by a surface relief that indicates a shape change resulting from slip or twinning, as can be observed in Figure 7c. Thus, the 17Mn-1Al steel possesses dual phases of martensite and retained austenite. However, optical microscopy is not effective to characterize this kind of structure, so observations are only qualitative.

Figure 8 shows that the constituent phases of the HMnS after hot forged and air-cooled examined by XRD are mainly austenite for the 22Mn-1.5Al and 22Mn-1Al steels. However, the steels with the lower manganese contents showed a dual phase of martensite and retained austenite. The X-ray diffraction measurements match the optical microscopy results.

Figure 9 shows a micrograph of the 22Mn-1.5Al steel showing the austenitic microstructure with

twins, NMIs, and micro-porosities. A homogeneous distribution of the chemical elements that constituted the matrix steel is observed. It was also observed for the four steels a relationship between NMIs which are formed by  $\text{Al}_2\text{O}_3$  and MnS particles.

### 3.3. Mechanical properties

Samples of the as-cast and hot-forged HMnS were obtained to evaluate the mechanical tests of hardness and tensile strength. The Rockwell B hardness for the as-cast and hot forged conditions is shown in Table 3.

It is observed from Table 3 that the hardness results remain constant for the as-cast condition and after the hot forging treatment of the HMnS evaluated. The hardness results are related to the amount of carbon, NMIs, and phases contained in the matrix. In addition, the low carbon content in the steels samples, and the similar content of NMIs for the as-cast condition and after the hot forging treatment, allow for obtaining hardness values in the range from 82 to 85 HRB, which fits with the results reported of 98 to 100 HRB for high-manganese steels with higher carbon contents (1 and 1.2 wt. % C) [41, 42]. A low hardness of 11.5 HRC was reported for 20Mn-3Al steel containing 1 wt% C. The low hardness was attributed to a matrix dominated by the dendrite of Fe-

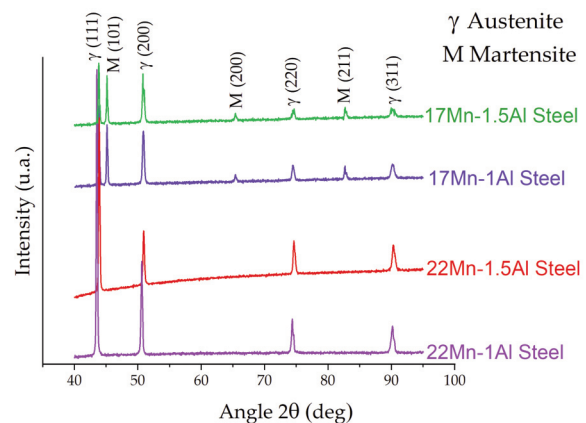


Figure 8. X-ray diffraction patterns corresponding to the HMnS in the hot forging condition

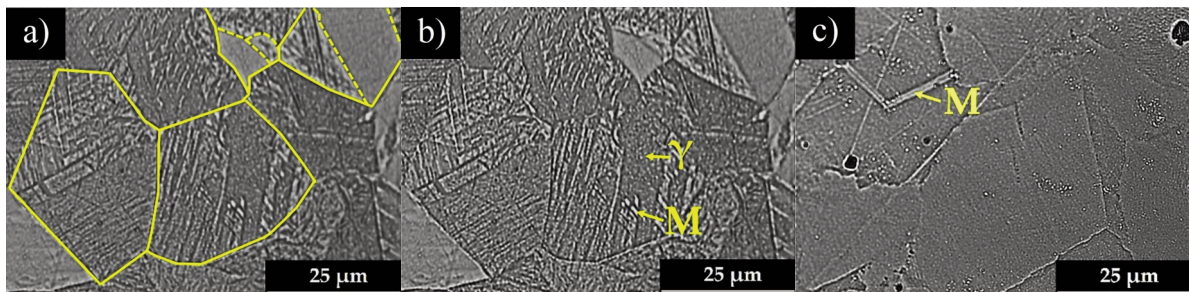


Figure 7. Microstructure of the 17Mn-1Al steel using OM showing a) grains (solid lines) and subgrains (dashed lines), b) martensite laths, and c) a surface relief of martensite

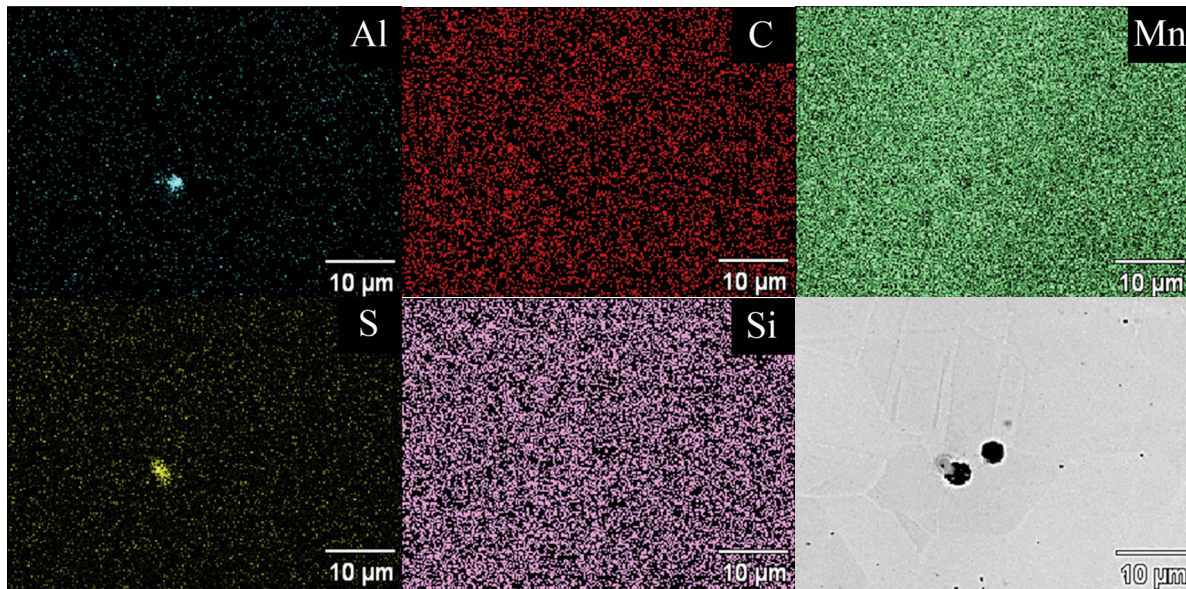


Figure 9. SEM micrograph and EDS analysis of the deformed 22Mn-1.5Al steel

Table 3. Hardness Rockwell B for the as-cast and hot forging conditions of the HMnS steels

Steel	Hardness (HRB)	
	As-cast	Hot forged
17Mn-1.5Al	82 ± 2.0	82 ± 2.3
17Mn-1Al	82 ± 2.0	83 ± 2.0
22Mn-1.5Al	85 ± 2.5	84 ± 2.2
22Mn-1Al	84 ± 2.1	83 ± 2.3

Al-C structure and austenite matrix. Therefore, the hardness results are mainly attributed to a solid solution hardening by the low aluminum content in an austenitic matrix [5]. The hardness results show that the hot forging treatment does not affect the hardness due to the formation of retained austenite as the main phase in the HMnS evaluated. This behavior could be beneficial for the machinability of these steels in engineering applications. It has been reported that HMnS (20-21 wt. % Mn) required a subsequent homogenization treatment of 1150 °C and 5 h to be processed [43].

However, the hot forging process in the HMnS allows the formation of twins and a duplex microstructure of martensite-austenite in the HMnS that contains the lowest amounts of manganese, which impacts the behavior of the tensile properties. Tensile tests were carried out for the four high-manganese steels in the as-cast condition and after the hot forging process. A series of engineering stress-strain curves obtained during tensile tests of the HMnS in the as-cast and hot forged conditions are shown in Figure 10. The values of yield strength ( $\sigma_{0.2}$ ), ultimate tensile strength ( $\sigma_{UTS}$ ), and total elongation ( $\delta$ ) are

represented in Table 4.

The yield strength was kept almost constant for the four steels samples at around 300 MPa, while the ultimate tensile strength reached values from 421 to 487 MPa in the as-cast condition. On the other hand, the total elongation of the as-cast steels does not exceed 13 %. In general, the mechanical properties of the tensile test were almost constant for the HMnS in the as-cast condition. The effect of adding aluminum was evident for the 22Mn-1.5Al steel where the highest yield strength was reached. Aluminum raises yield stress by solid solution hardening increasing both SFE and matrix strength [44].

It is observed that the hot forging treatment leads to a significant increase in the strength of the HMnS from the as-cast condition, reaching values in the range of 345 to 544 MPa and from 754 to 971 MPa for the yield and ultimate tensile strengths, respectively. The highest strength results were obtained for the 17Mn-1Al steel. The results show that elongation was kept almost constant for the deformed steels. The low additions of aluminum evaluated in the HMnS did not show a significant change in the tensile properties. Although the 17Mn-1.5Al and 17Mn-1Al steels formed a dual microstructure of retained austenite and martensite; in general, the total elongation of the steels remained almost constant for the four steel samples evaluated. Mechanical twins cause the strengthening of the material because they constitute strong barriers to the dislocation slip while martensite causes fragmentation and refinement of the microstructure, leading to the hardening of the HMnS [45].

The UTS and elongation are strongly related to alloying elements such as manganese and aluminum. As was observed from figure 6, when manganese

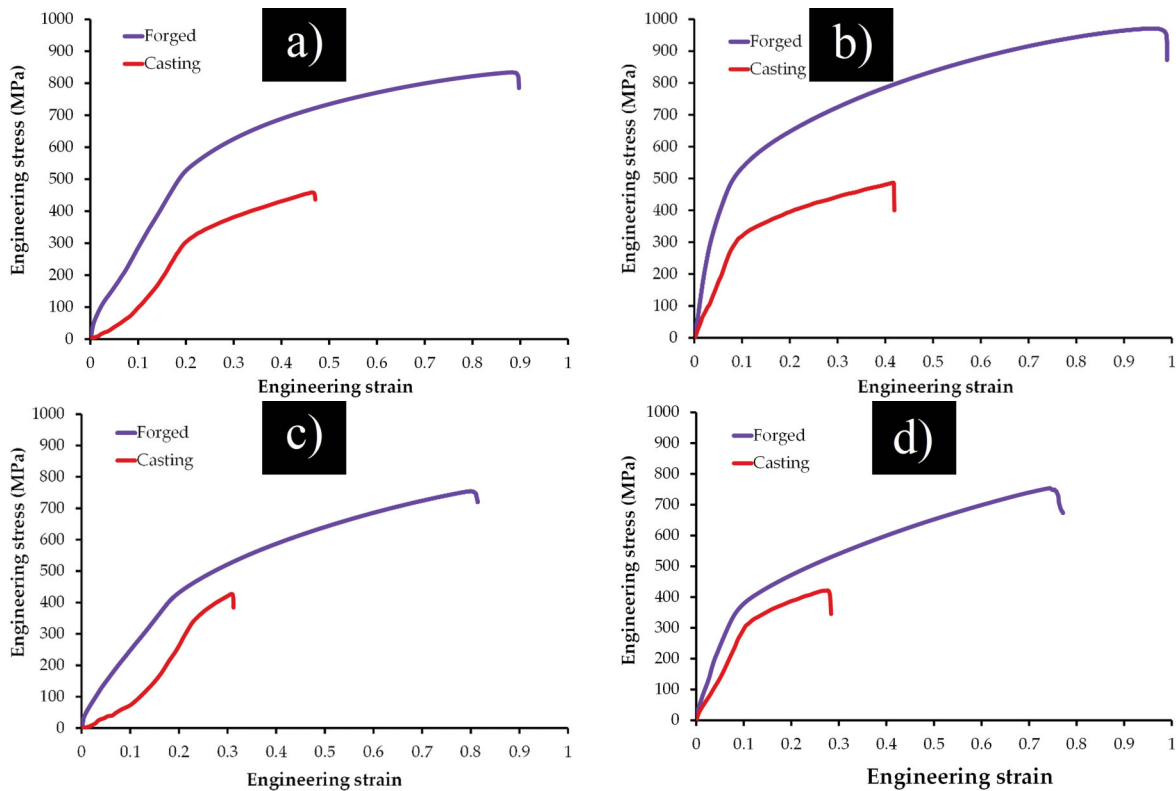


**Figure 10.** Engineering stress–strain curves of the as-cast and deformed HMnS for a) 17Mn-1.5Al, b) 17Mn-1Al c) 22Mn-1.5Al, d) 22Mn-1Al

**Table 4.** The yield strength ( $\sigma_{0.2}$ ), ultimate tensile strength ( $\sigma_{UTS}$ ), and total elongation ( $\delta$ ) of the HMnS

Steel	Condition	( $\sigma_{0.2}$ ), MPa	( $\sigma_{UTS}$ ), MPa	( $\delta$ ), %
17Mn-1.5Al	As-cast	315 ± 11	458 ± 29	13 ± 2
	Hot forged	544 ± 39	833 ± 22	24 ± 2
17Mn-1Al	As-cast	311 ± 2	487 ± 7	12 ± 1
	Hot forged	496 ± 20	971 ± 49	26 ± 2
22Mn-1.5Al	As-cast	334 ± 7	426 ± 25	9 ± 1
	Hot forged	345 ± 10	756 ± 45	20 ± 2
22Mn-1Al	As-cast	321 ± 22	421 ± 19	9 ± 2
	Hot forged	372 ± 3.5	754 ± 76	21 ± 3

increased from 17 to 21 wt%, the grain size increased twice and the UTS and elongation decreased. Therefore, a larger amount of grain boundaries provide a great number of barriers to dislocation movement, increasing the strength of the material. Besides, when the aluminum content increased from 1.0 to 1.5 wt%, the UTS and elongation decreased because of the increase in the NMIs content that aided the crack propagation during the tensile test [40]. U. Gürol et al [46], reported that by increasing manganese content from 13 wt% to 17 wt%, the stacking fault energy was increased, and thus, the

shear stress needed for sliding increased, this least contributes to increasing UTS and elongation. However, when the manganese content increased to 21 wt%, the grain size increased almost two times and as a consequence, the UTS and elongation decreased.

The strength of the steels is related to their microstructure and the type and non-metallic inclusions content. As inclusions inside the material act like stress raisers in the matrix, the crack initiation and propagation during the internal fracture are affected by the non-metallic inclusion features such as content, size, and inclusion type [47]. Despite the vacuum applied during the steels manufacturing, there was the formation of endogenous inclusions; however, no elongation of the MnS inclusions was observed after the hot forging process. Thus, there was no anisotropy in mechanical properties. In general, a decrease in the grain size allows for an increase in the strength of the steel. The 17Mn-1Al steel showed the smallest grain size and the finer NMIs homogeneously distributed in the matrix along together with the dual microstructure led to obtaining the higher mechanical properties of strength and elongation. It has been reported [48] that carbide inclusion can be used to strengthen austenitic manganese steel if it is not allowed to exceed the optimum size that can impede dislocation movement and is also not allowed to diffuse into the grain

boundaries which might lead to embrittlement. For these conditions, NMIs can be considered as precipitation-strengthening mechanisms that can be used in improving the wear resistance of HMnS for service conditions where abrasive loading is required. The mechanical properties obtained in this study are located between those obtained for high manganese steels and advanced steels of the second generation [49]. The parameters used of short homogenization time and air cooling during the hot forging treatment allowed to obtain recrystallized grains of annealing twins and martensite in a retained austenite matrix. The microstructure obtained allows for obtaining the highest strength of the 17Mn-1Al steel without an increase in hardness, which may be beneficial in the production of this type of HMnS. Despite the attractive properties obtained by the HMnS as major structural material mainly for automotive industry applications, some concerns have been attempted to address these steels, such as their poor wet corrosion resistance due to the high dissolution rate of Mn. In addition, NMIs act as localized corrosion initiation and propagation for these steels; therefore, the evaluation of other chemical elements is carried out to enhance the corrosion properties of the HMnS [7, 50]. The manufacturing process by continuous casting and hot strip rolling of these steels is another challenge to be treated due to segregation problems and particle precipitation during solidification [36].

The mechanical properties of high-manganese steels are very dependent on carbon and manganese contents [46]. The low carbon content in the studied steels allows for obtaining low hardness values as was previously reported for Hadfield and high-manganese steels [4, 5, 7]. In addition, carbide particles were not formed which may increase hardness. However, the hot forging process for the HMnS containing 17 wt% Mn and the higher non-metallic inclusion contents allow for refining the microstructure of the HMnS obtaining smaller equiaxed grains of retained austenite, characterized by a duplex structure of austenite retained and martensite which cause a strengthening of the material. Martensite presents different orientations and hence effective barriers to slip due to carbon atoms and high dislocation density [51], dislocations should change their direction for their movement requiring more energy, increasing the yield and tensile strength. The HMnS containing 22 wt% Mn showed a microstructure of retained austenite grains containing twins. The twins induce deformation due to the twin boundaries acting as strong barriers to dislocation motion, which leads to an increase in the strength and elongation of the steels [48]. However, the equiaxed grain sizes were bigger than HMnS with 17 wt% Mn obtaining lower mechanical results.

#### 4. Conclusions

HMnS with low aluminum contents were manufactured and characterized by microstructural and mechanical tests. The results obtained can be summarized as follow:

1. The as-cast steels produced consisted of an austenitic matrix and finer non-metallic inclusions of  $Al_2O_3$  and MnS homogeneously distributed in the steels. Increasing the aluminum content in the HMnS increased the amount of NMIs.

2. Hot forging promoted a recrystallized microstructure of equiaxed grains consisting of annealing twins in a retained austenite matrix in the steels with 22 wt% Mn, while a duplex microstructure of retained austenite and low amounts of martensite was obtained in the steels with 17 wt% Mn.

3. The hardness of the steels was similar to that obtained in the as-cast and deformed conditions reaching values in the range of 82 to 85 HRB, since the low concentration of carbon and aluminum and the high concentration of manganese allowed a completely austenitic microstructure without carbides.

4. The highest tensile values were obtained for the relatively low manganese 17Mn-1Al steel, as the austenite and martensite microstructure was maintained with the highest amount of NMIs homogeneously distributed in the steel matrix, which aid in the grain size refining after the hot forging process.

#### Acknowledgments

*The authors wish to thank Institutions CONACyT, SNI, COFAA, and SIP-Instituto Politécnico Nacional. A. Cruz appreciates the support of the company Multico and Engineers Ricardo Balver and Jaime Téllez for the hot forging tests.*

#### Author Contributions

*Data curation, Erick Morales Cruz and José Martínez Vázquez; Formal analysis, Marissa Vargas Ramírez, Eduardo Colin García, and Alejandro Cruz Ramírez; Funding acquisition, Azdrubal Lobo Guerrero, Marissa Vargas Ramírez, and José Martínez Vázquez; Investigation, Eduardo Colin García, Erick Morales Cruz, and Alejandro Cruz Ramírez; Methodology, Eduardo Colin García, Víctor Hugo Gutiérrez Pérez, and Ricardo Sánchez Alvarado; Project administration, Marissa Vargas Ramírez; Visualization, Alejandro Cruz Ramírez, Marissa Vargas Ramírez and Eduardo Colin García; Writing - original draft, Alejandro Cruz Ramírez; Writing - review & editing, Alejandro Cruz Ramírez and Eduardo Colin García. All authors have read and*



agreed to the published version of the manuscript.

### Data Availability Statement

No additional data

### Conflicts of Interest

The authors declare no conflict of interest

### References

- [1] G. Frommeyer, U. Brux, P. Neumann, Supra-ductile and high-strength manganese-TRIP/TWIP steels for high energy absorption purposes, *ISIJ International*, 43 (2003) 438-446. <https://doi.org/10.2355/ISIJINTERNATIONAL.43.438>
- [2] G. Frommeyer, U. Brux, Microstructures and mechanical properties of high-strength Fe-Mn-Al-C light-weight TRIPLEX steels, *Steel Research International*, 77 (2006) 627-633. <https://doi.org/10.1002/srin.200606440>
- [3] A. Tomaszewska, M. Jablonska, G. Niewielsky, R. Kawalla, E. Hadasik, Research of selected properties of two types of high manganese steel wires. *IOP Conference Series Materials Science and Engineering*, 22 (2011) 012015. doi:10.1088/1757-899X/22/1/012015
- [4] O. Cobos O, A. Romero, M. Monsalve, Cooling kinetics effect on abrasive wear behavior of an ASTM A128 steel, *Contemporary Engineering Sciences*, 11 (71) (2018) 3531-3537. <https://doi.org/10.12988/ces.2018.87362>.
- [5] K. Panchal, Life improvement of Hadfield manganese steel castings. *International Journal of Scientific Development and Research*, 5 (1) (2016) 817-825. <http://www.ijedr.org/papers/IJSDR1605148.pdf>.
- [6] A. Srivastava, K. Das, Microstructural characterization of Hadfield austenitic manganese steel, *Journal of Materials Science*, 43 (2008) 5654-5658. <https://doi.org/10.4236/jmmce.2013.15042>.
- [7] S. Ayadi, A. Hadji, Effect of chemical composition and heat treatments on the microstructure and wear behavior of manganese Steel, *International Journal of Metalcasting*, (2020). <https://doi.org/10.1007/s40962-020-00479-2>.
- [8] J. Jin, Y. Lee Y, Effects of Al on microstructure and tensile properties of C-bearing high Mn TWIP Steel, *Acta Materialia*, 4 (60) (2012) 1680-1688. <https://doi.org/10.1016/j.msea.2018.02.003>.
- [9] A. Ghosh, Secondary steelmaking: principles and applications, CRC Press LLC: USA, 2001, p. 255.
- [10] D. Matlock, J. Speer, E. Moor, P. Gibbs, Recent developments in advanced high strength sheet steels for automotive: An overview, *JESTECH*, 15 (1) (2012) 1-12.
- [11] S. Kim, G. Kim G, K. Chin, Development of high manganese TWIP steel with 980 MPa tensile strength, *Proceedings of the International Conference of New Developments in Advanced High-Strength Sheet Steels*, AIST, Orlando Fl. (2008) 249-256.
- [12] S. Lee, B. Cooman, Tensile behavior of intercritically annealed ultra-fine grained 8% Mn multi-phase steel, *Steel Research International*, 10 (8) (2015) 1170-1178. <https://doi.org/10.1002/srin.201500038>.
- [13] T. Brune T, D. Senk, R. Walpot, B. Steennken, Hot ductility behavior of Boron containing microalloyed steels with varying manganese contents, *Metallurgical and Materials Transactions B*, 46 (2015) 1400-1408. <https://doi.org/10.1007/s11663-015-0306-1>.
- [14] X. Yang, L. Zhang, C. Lai, S. Li S, M. Li, Z. Deng, A method to control the transverse corner cracks on a continuous casting slab by combining microstructure analysis with numerical simulation of the slab temperature field, *Steel Research International*, 1700480 (89) (2018) 1-8. <https://doi.org/10.1002/srin.201700480>.
- [15] S. Sant, R. Smith, A study in the work-hardening behaviour of austenitic manganese steels, *Journal of Materials Science*, 22 (1987) 1808-1814. <https://doi.org/10.1007/BF01132410>.
- [16] F. Chen, C. Chou C, P. Li, S. Chu, Effect of aluminium on TRIP Fe Mn Al alloy steels at room temperature, *Materials Science and Engineering A*, 160 (2) (1993) 261-270.
- [17] Y. Han, S. Hong, The effect of Al on mechanical properties and microstructures of Fe-32Mn-12Cr-xAl-0.4C cryogenic alloys, *Materials Science and Engineering A*, 222 (1) (1997) 76-83.
- [18] S. Takaki, T. Furuya, Y. Tokunaga, Effect of Si and Al additions on the low temperature toughness and fracture mode of Fe-27Mn alloys, *ISIJ International*, 30 (1990) 632-638. <https://doi.org/10.2355/isijinternational.30.632>.
- [19] R. Gurumayum, L. Yi-Jyun, Ch. Wei-Chun, Evidence of martensitic transformation in Fe-Mn-Al steel similar to maraging Steel, *Metallurgical and Materials Transactions A*, 52 (2021) 26-32. <https://doi.org/10.1007/s11661-020-06054-y>.
- [20] L. Kučerová, H. Jirková, J. Volkmanová, J. Vrtáček, Effect of aluminium and manganese contents on the microstructure development of forged and annealed TRIP Steel, *Manufacturing Technology*, 18 (4) (2018) 605-610. <https://doi.org/10.21062/ujep/146.2018/a/1213-2489/MT/18/4/605>.
- [21] V. Flaxa, J. Shaw, Material Application in ULSAB-AVC, *Steel Grips*, 1 (4) (2003) 255-261.
- [22] M. Mehrkens, J. Fröber, Modern multi-phase steels in the BMW of the Porsche Cayenne, *Steel Grips*, 1 (4) (2003) 249-251.
- [23] G. Frommeyer, O. Grässel, High strength TRIP-TWIP and superplastic steels development, properties, application, *La Revue de Metallurgie-CIT*, 10 (1998) 1299-1310.
- [24] S. Allain, J. Chateau, O. Bouaziz, S. Migot, N. Guelton, Correlations between the calculated stacking fault energy and the plasticity mechanisms in Fe-Mn-C alloys, *Materials Science and Engineering A*. 387-389 (2004) 158-162. <https://doi.org/10.1016/j.msea.2004.01.059>.
- [25] R. Ueji, N. Tsuchida, D. Terada, N. Tsuji, Y. Tanaka, A. Takemura, K. Kunishige, Tensile properties and twinning behavior of high manganese austenitic steel with fine-grained structure. *Scripta Materialia*, 59 (9) (2008) 963-966. <https://doi.org/10.1016/j.scriptamat.2008.06.050>.
- [26] Y. Estrin, H. Mecking, A unified phenomenological description of work hardening and 26 creep based on



- one-parameter models, *Acta Metallurgica et Materialia*, 32 (1984) 57-70.
- [27] O. Bouaziz, S. Allain, C. Scott, P. Cugy, D. Barbier, High manganese austenitic twinning induced plasticity steels: A review of the microstructure properties relationships, *Solid State and Materials Science*, 15 (2011) 141-168. <https://doi.org/10.1016/j.cossms.2011.04.002>.
- [28] T. Furuhashi, N. Kimura, T. Maki, Proceedings 1st International Conference on High Mn steel, The Korean Institute of Metals and Materials, Seoul, Korea, May 2011.
- [29] K. Chin, Automotive-Circle, 12. Proceedings International Conference on Materials in car body engineering, Bad Nauheim, Germany, May 2010.
- [30] R. Van Tol, L. Zhao, J. Sietsma, Proceedings 1st International Conference on High Mn steel, The Korean Institute of Metals and Materials, Seoul, Korea, May 2011.
- [31] A. Hamada, L. Karjalainen, M. Somani, The influence of aluminium on hot deformation behaviour and tensile properties of high-Mn TWIP steels, *Materials Science and Engineering A*, 467 (1-2) (2007) 114-124. <https://doi.org/10.1016/j.msea.2007.02.074>.
- [32] C. Igathinathane, L. Pordesimo, E. Columbus, E. Batchelor, S. Methuku, Shape identification and particle size distribution from basic shape parameters using ImageJ, *Computers and Electronics in Agriculture*, 63 (2008) 168-182. <https://doi.org/10.1016/j.compag.2008.02.007>.
- [33] B. De Cooman, O. Kwon, K. Chin, State-of-the-knowledge on TWIP Steel, *Materials Science and Technology*, 28(5) (2012) 513-527. <https://doi.org/10.1179/1743284711Y.0000000095>.
- [34] G. Reyes, A. Cruz, E. Colin, V. Gutiérrez, Thermodynamic analysis of the graphite flake formation of low manganese and sulfur gray cast iron, *Archives of Metallurgy and Materials Science*, 66 (1) (2021) 249-258. <https://doi.org/10.24425/amm.2021.134782>.
- [35] N. NguyenVan, K. Kato, H. Ono, Precipitation Behavior of AlN Inclusions in Fe-0.5Al-2.0Mn alloy under continuous unidirectional solidification process, *Frontiers in Materials*, 8 (736284) (2021) 1-8. <https://doi.org/10.3389/fmats.2021.736284>.
- [36] T. Allam, W. Bleck, C. Klinkenberg, B. Kintscher, U. Krupp, J. Rudnizki, The continuous casting behavior of medium manganese steels, *Journal of Materials Research and Technology*, 15 (2021) 292-305. <https://doi.org/10.1016/j.jmrt.2021.08.019>.
- [37] L. Zhang, B. Thomas, X. Wang, K. Cai, Evaluation and control of steel cleanliness - Review, 85th Steelmaking Conference Proceedings, ISS-AIME, Warrendale, PA, 2002.
- [38] Y. Lee, J. Han, Current opinion in medium manganese steel, *Materials Science and Technology* 31(7) (2015) 843-856. <https://doi.org/10.1179/1743284714Y.0000000722>.
- [39] G.S. Rohrer, Introduction to grains, phases, and interfaces-an interpretation of microstructure, *Trans AIME*, 175 (1948) 15-51. <https://doi.org/10.1007/s11661-010-0215-5>.
- [40] Z. Wu, W. Zheng, G. Li, H. Matsuura, F. Tsukihashi, Effect of inclusions behavior on the microstructure in Al-Ti deoxidized and Magnesium-Treated steel with different aluminum contents, *Metallurgical and Materials Transactions B*, 46 (2015) 1226-1241. <https://doi.org/10.1007/s11663-015-0311-4>.
- [41] L. Qian, X. Feng, F. Zhang, Deformed microstructure and hardness of Hadfield high manganese steel, *Materials Transactions* 52 (8) (2011) 1623-1628. <https://doi.org/10.2320/matertrans.M2011121>.
- [42] Y. Wen, H. Peng, H. Si, R. Xiong, D. Raabe, A novel high manganese austenitic steel with higher work hardening capacity and much lower impact deformation than Hadfield manganese Steel, *Materials & Design*, 55 (2014) 798-804. <https://doi.org/10.1016/j.matdes.2013.09.057>.
- [43] B. Wietbrock, M. Bambach, S. Seuren, G. Hirt, Homogenization strategy and material characterization of high-manganese TRIP and TWIP steels, *Materials Science Forum*, 638-642 (2010) 3134-3139. <https://doi.org/10.4028/www.scientific.net/MSF.638-642.3134>.
- [44] O. Grässel, G. Frommeyer, C. Derder, H. Hofmann, Phase transformations and mechanical properties of Fe-Mn-Si-Al TRIP-Steels, *Journal of Physics: IVP Proceedings, EDP Sciences*, 7 (C5) (1997) 383-388. <https://hal.archives-ouvertes.fr/jpa-00255657>.
- [45] J. Kowalska, J. Ryś, G. Cempura, Complex structural effects in deformed high-manganese Steel, *Materials*, 14 (6935) (2021) 1-19. <https://doi.org/10.3390/ma14226935>.
- [46] U. Gürol, S. Can Kurnaz, Effect of carbon and manganese content on the microstructure and mechanical properties of high manganese austenitic steel, *Journal of Mining and Metallurgy Section B-Metallurgy* 56 (2) (2020) 171-182. <https://doi.org/10.2298/JMMB191111009G>.
- [47] R. Arreola, A. Cruz, J. Rivera, A. Romero, R. Sánchez, The effect of non-metallic inclusions on the mechanical properties of 32 CDV 13 steel and their mechanical stress analysis by numerical simulation, *Theoretical and Applied Fracture Mechanics*, 94 (2018) 134-146. <https://doi.org/10.1016/j.tafmec.2018.01.013>.
- [48] F. Bahfie, B. Aji, F. Nurjaman, A. Junaedi, E. Sururiah, The effect of aluminum on the microstructure and hardness of high austenitic manganese Steel, *IOP Conference Series Materials Science and Engineering*, 285 (012020) (2018) 1-4. <https://doi.org/10.1088/1757-899X/285/1/012020>.
- [49] G. Dini, A. Najafzadeh, R. Ueji, S. Monirvaghefi, Improved tensile properties of partially recrystallized submicron grained TWIP Steel, *Materials Letters*, 64 (1) (2011) 15-18. <https://doi.org/10.1016/J.MATLET.2009.09.057>.
- [50] J. Hajšman, L. Kucerová, K. Burdová, The Influence of varying aluminium and manganese content on the corrosion resistance and mechanical properties of high strength steels, *Metals*, 11 (9) (2021) 1-16. <https://doi.org/10.3390/met11091446>.
- [51] George E. Dieter, *Mechanical metallurgy*, Mc-Graw Hill, Boston, Massachusetts, 1986, 185-188 and 227-229.



## UTICAJ DODAVANJA NISKIH KOLIČINA ALUMINIJUMA NA MIKROSTRUKTURU I MEHANIČKE OSOBINE VRUĆE KOVANIH ČELIKA SA VISOKIM SADRŽAJEM MANGANA

E.U. Morales-Cruz <sup>a</sup>, M. Vargas-Ramírez <sup>a</sup>, A. Lobo-Guerrero <sup>a</sup>, A. Cruz-Ramírez <sup>b,\*</sup>, E. Colin-García <sup>b</sup>, R.G. Sánchez-Alvarado <sup>b</sup>, V.H. Gutiérrez-Pérez <sup>c</sup>, J.M. Martínez-Vázquez <sup>d</sup>

<sup>a</sup> Autonomni univerzitet u Idalgu -UAEH, Odsek za proučavanje materijala, Pačuka, Meksiko

<sup>b</sup> Nacionalni politehnički univerzitet- ESIQIE, Odsek za inženjerstvo u metalurgiji i materijalima, Sijudad de Meksiko, Meksiko

<sup>c</sup> Nacionalni politehnički univerzitet- UPIIZ, Odeljenje za specifično stručno osposobljavanje, Zakatekas, Meksiko

<sup>d</sup> Politehnički univerzitet Juventino Rosas - UPJR, Guanahuato, Meksiko

### Apstrakt

U ovom radu analiziran je uticaj malih dodataka aluminijuma i procesa vrućeg kovanja na mikrostrukturu i nemetalne uključke visokomanganskih čelika. Četiri čelika sa visokim sadržajem mangana (HMnS) pripremljena su tako što je u četiri austenitna čelika sa srednjim sadržajem ugljenika (0,3-0,4 tež.% C) i sadržajem mangana od 17 i 22 tež.% dodat niski sadržaj aluminijuma od 1,1 i 1,5 tež.% Uzorci od livenog čelika su vruće kovani na 1100 °C da bi se postigla ukupna redukcija od 70%. Mikrostrukturna evolucija je izvedena primenom mikroskopskih tehnika (OM i SEM-EDS) i merenja difrakcije rendgenskih zraka za livene i vruće kovane čelike. Tipična zrnasta stubna zona formirana tokom očvršćavanja livenog ingota je dobijena u stanju livenja, gde se mikrostruktura sastojala od nemetalnih uključaka u potpuno austenitnoj matrici. Nemetalni uključci su identifikovani kao čestice  $Al_2O_3$  i MnS. Termomehanička obrada omogućava formiranje austenitne mikrostrukture koju karakterišu dvojnikanje u čelicima sa visokim sadržajem mangana, dok je austenitno-martenzitna dupleks mikrostruktura dobijena u HMnS, koja je imala najmanji sadržaj mangana. Najveće vrednosti zatezne čvrstoće dobijene su za čelik 17Mn-1Al, koji je imao najmanju veličinu zrna i veći sadržaj nemetalnih uključaka. Vrednosti tvrdoće su bile slične onima dobijenim u livenom stanju.

**Ključne reči:** Čelik; Vruće kovanje; Mangan; Hadfield; Mikrostruktura

